Recognition in the Minor Groove of Double-Stranded DNA by Microgonotropens

ALEXANDER L. SATZ AND THOMAS C. BRUICE*

Department of Chemistry, University of California, Santa Barbara, California 93106

ABSTRACT

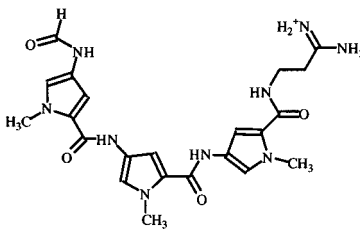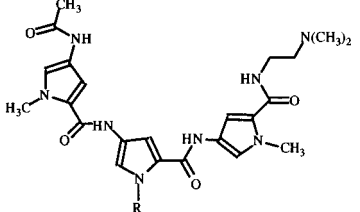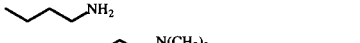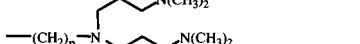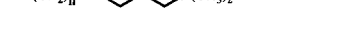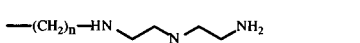Microgonotropens consist of a minor groove binding moiety functionalized with alkylamine side chains which are protonated and positively charged at neutral pH and capable of forming electrostatic bonds with the negatively charged phosphodiester backbone of DNA. We have investigated the interactions between microgonotropens and double-stranded DNA by a combination of fluorescence, ultraviolet, and nuclear magnetic resonance spectroscopy. Our work reveals why microgonotropens are such potent inhibitors of the binding of transcription factors to their DNA binding sites.

Introduction

When expressed incorrectly, specific genes whose protein products are essential for the regulation of cell growth result in cancer.[1] DNA binding agents have been shown to influence the regulation of gene expression by inhibiting the binding of transcription factors (TFs) to their dou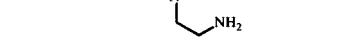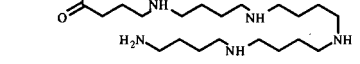ble-stranded DNA (dsDNA) binding sites.[2–4] Interest in controlling the expression of specific genes has spurred efforts toward the development of DNA binding agents with greater sequence selectivity and a more potent ability to disrupt TF–dsDNA interactions.[4,5] Small molecules which bind to the minor groove (MGBs) are practical lead compounds for the development of new anticancer agents because they often localize in the nuclear DNA of whole cells and possess a track record of promising biological activity.[6,7] For instance, distamycin[7] and the duocarmycins[8] are naturally occurring antibiotics, and Hoechst 33258 is fairly effective as an anthelminthic.[9]

Structural Motifs. Commonly the development of novel MGBs employs the structural motifs presented by the tripyrrole polyamide of distamycin (Table 1) or the bisbenzimidazole of Hoechst 33258 (Table 2). Distamycin and Hoechst 33258 possess crescent shapes matching the

Table 1. Association Constants for Tripyrrole Polyamide Compounds with d(GGCGA₃T₃GGCGG)/ d(CCGCCA₃T₃CGCC) (D1) in H₂O, 10 mM Phosphate Buffer, pH 7.0/10 mM NaCl at 35 °C

structure		$\log(K_3K_4)^a$
	distamycin	16.0
	MGTs	
	L1	13.0
	L2	16.4
	L3 (n = 3)	17.3
	L4 (n = 4)	17.3
	L5 (n = 5)	17.2
	L6 (n = 3)	18.4
	L7 (n = 4)	17.9
	L8	16.7
	L9	17.3

^{a} K_3 and K_4 are defined in Scheme 1.

curvature of the minor groove of dsDNA and selectively bind sequences of four contiguous A + T base pairs with nanomolar dissociation constants.[7,10] The polymeric polyamide motif lends itself to rapid solid phase synthesis.[11,12] Bisbenzimidazoles form fluorescent complexes with dsDNA, which facilitates investigation of their binding.[6,13]

Figure 1A provides a schematic of a characteristic antiparallel side-by-side binding motif composed of two tripyrrole polyamides. Figure 1B depicts a characteristic "simple" 1-to-1 binding motif of a bisbenzimidazole.[7,14,15] Complexion of dsDNA by a tripyrrole or a bisbenzimidazole induces little change in the conformation of the helix.[16] Thus, minor groove binding of dsDNA by such molecules can occur simultaneously with triple helix formation[17] or complexation by a major groove binding protein.[18] Still, MGBs do influence some protein–dsDNA interactions, as shown by their ability to inhibit transcription.[2,6]

Alexander L. Satz carried out undergraduate research in photochemistry under the direction of Prof. Peter R. Ogilby at the University of New Mexico, where he received his B.S. degree in 1996. Dr. Satz obtained his Ph.D. in 2001 under the direction of Prof. Thomas C. Bruice at the University of California, Santa Barbara. Dr. Satz is currently conducting his postdoctoral studies in the research group of Prof. Robert R. Rando at Harvard Medical School.

Thomas C. Bruice dropped out of high school in the eleventh grade (1943) to serve in the military. He attended the University of Southern California (B.S., 1950; Ph.D., 1954) and received his postdoctoral training at UCLA. Prior to joining the faculty of the University of California at Santa Barbara in 1964, Professor Bruice held faculty positions at Yale, John Hopkins, and Cornell Universities. An inventor of the term "bioorganic chemistry", he has contributed importantly to many areas of mechanistic chemistry dealing with problems important in biochemistry.

Table 2. Increase in Melting Temperatures for 0.80 μM d(GCGACTGCA$_2$T$_3$CGACGTCC)/ d(GGACGTCGA$_3$T$_2$GCAGTCGC) (D3) in the Presence of 2.8 μM Bisbenzimidazoles in H$_2$O, 10 mM Phosphate Buffer, pH 7.2/10 mM NaCl[a]

structure		$t_m - t^0_m$
L10		+5
L11		+22
L12		+26
L13 (n = 1)		+21
L14 (n = 3)		+22
Hoechst-33258		+10

[a] t_m and t_m^0 are melting temperatures for **D3** with and without the presence of bisbenzimidazole, respectively.

Our Approach. To increase the potency of tripyrrole polyamide or bisbenzimidazole-type molecules, numerous conjugates incorporating intercalating or alkylating moieties have been synthesized.[19] Our research group has pursued a complementary approach in developing a new class of agents we call microgonotropens (MGTs).[20] MGTs consist of a minor groove binding moiety functionalized with alkylamine side chains which are protonated and positively charged at neutral pH and capable of forming electrostatic bonds with the negatively charged phosphodiester backbone of DNA.[21,22] Our investigations have shown MGTs to possess beneficial characteristics, including (i) increased association constants for dsDNA complexation, (ii) the ability to induce gross conformational changes in dsDNA, and (iii) an improved ability to inhibit binding of dsDNA by TFs.

Tripyrrole Microgonotropens

Tripyrrole MGTs bear a protonated and positively charged alkylamine side chain extending from the N$_1$ position of one of the agent's three pyrrole rings (Table 1). Similar to distamycin,[10] DNase I footprint analysis of dsDNA after incubation with the MGTs showed protection at tracts containing at least four contiguous A + T base pairs.[21,22]

Association constants for complexation of d(GGCGCA$_3$-T$_3$GGCGG/d(CCGCCA$_3$T$_3$GCGCC) (**D1**, Chart 1) were determined by competition of MGT with Hoechst 33258 for the duplex's A$_3$T$_3$ binding site (see Figure 2).[23] The fluorescence emission from complexes of MGTs with **D1** is negligible compared to that from the strongly fluorescent complex of Hoechst 33258 with **D1**. Because the MGTs form 2-to-1 complexes with the A$_3$T$_3$ binding site, there exist two association constants, K_3 and K_4, one for each binding event (Scheme 1). In Table 1, the K_3 and K_4 values for the complexation of **D1** by ligand molecules is presented as the log of the value K_3K_4.
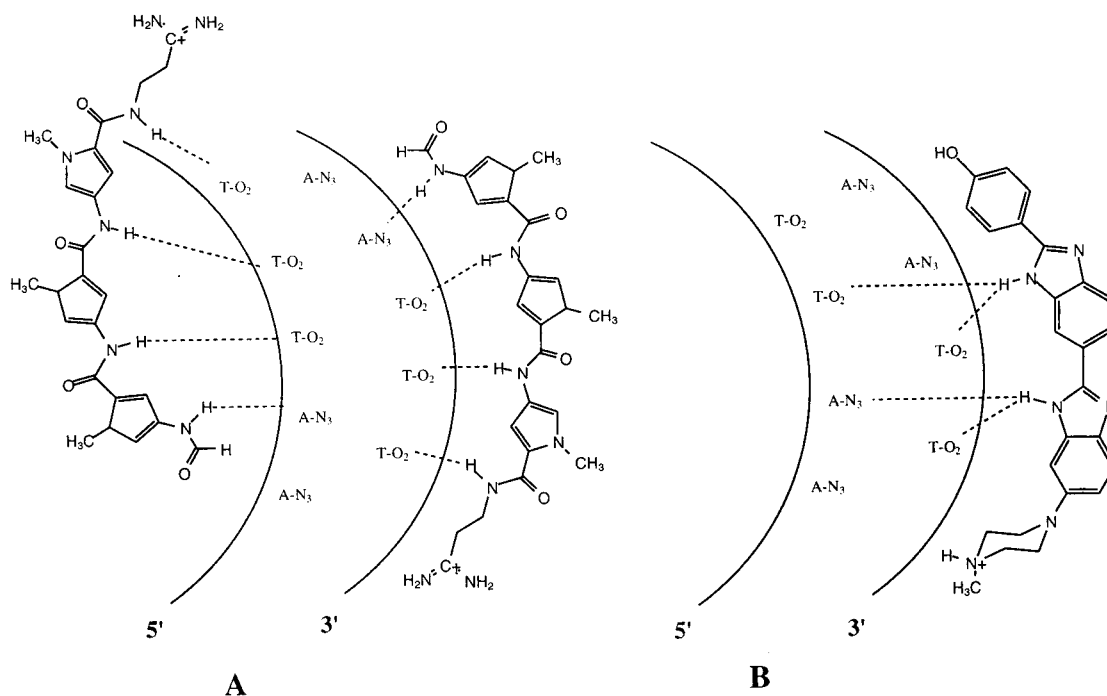
FIGURE 1. Schematic diagram of hydrogen bond interactions between MGBs and DNA. (A) An antiparallel side-by-side binding motif composed of two distamycin molecules. (B) A "simple" 1-to-1 binding motif between dsDNA and Hoechst 33258.

Chart 1

> **(D1)** d(GGCGCA$_3$T$_3$GGCGG)/
> d(CCGCCA$_3$T$_3$GCGCC)
>
> **(D2)** d(CGCA$_3$T$_3$GCG)$_2$
>
> **(D3)** d(GCGACTGCA$_2$T$_3$CGACGTCC)/
> d(GGACGTCGA$_3$T$_2$GCAGTCGC)
>
> **(D4)** d(CGCA$_5$CGCACC)/
> d(GGTGCGT$_5$GCG)
>
> **(D5)** d(CGCA$_9$CGC)/d(GCGT$_9$GCG)
>
> **(D6)** d(GCGGTATA$_4$TTCGACG)/
> d(CGTCGAAT$_4$ATACCGC)

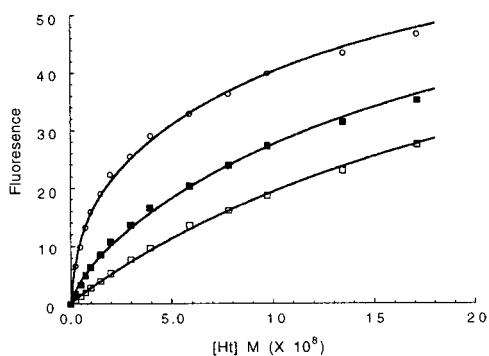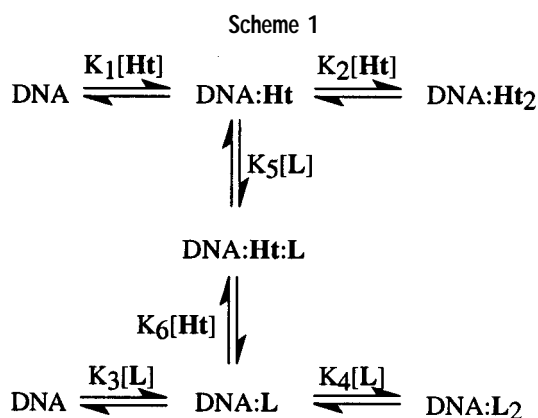**FIGURE 2.** Representative plots of fluorescence (*F*, in arbitrary units) versus total concentration of Hoechst 33258 for **L8** at 5 × 10^{-9} (○), 7.5 × 10^{-9} (■), and 1.0 × 10^{-8} M (□) in the presence of 5.0 × 10^{-9} M **D1**. The association constants K_3 and K_4 were determined by curve fitting[23] of the experimental data (Scheme 1).

Scheme 1

Formation of the (Hoechst 33258)$_2$:**D1** complex, as presented in Scheme 1, was observed by spectrofluorometric titration [log(K_1K_2) = 16.7 M^{-2} for Hoechst 33258, see Table 1 for conditions]. For the tripyrrole polyamides, which do not form fluorescent complexes with dsDNA, (L)$_2$:**D1** complexes were observed by employing spectrophotometric titrations. Additionally, formation of 2-to-1 stoichiometries for Hoechst 33258[22,24] and the tripyrrole polyamides **L5**[24] and **L7**[25] with **D1** was verified by ¹H NMR titrations (Chart 2, Table 1). Further, (distamycin)$_2$: d(CGCA$_3$T$_3$GCG)$_2$ (**D2**), and at high concentrations (dis-

Chart 2
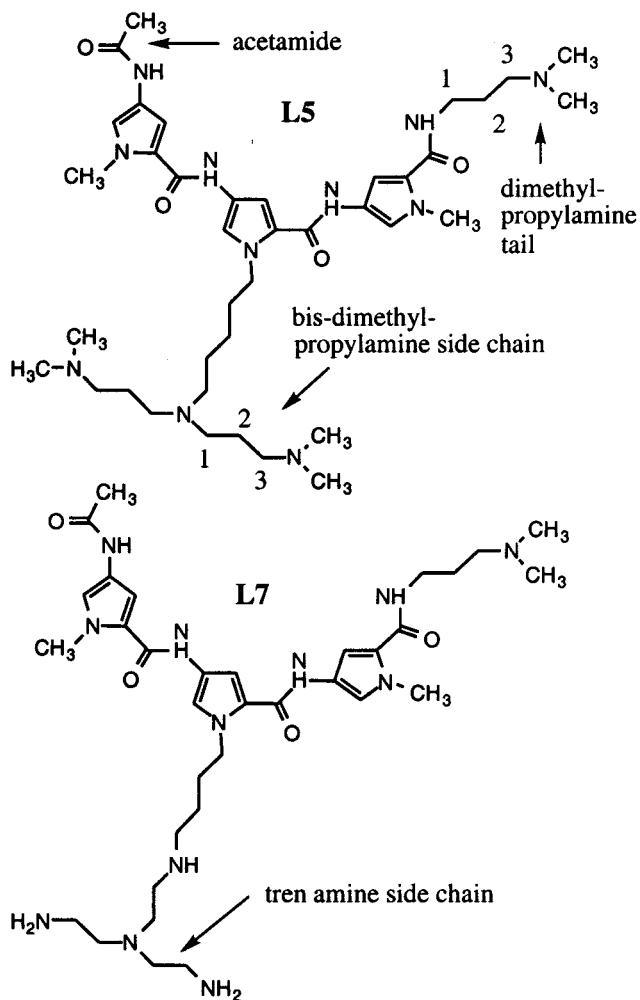
dsDNA D2

5'-C$_1$ G$_2$ C$_3$ A$_4$ A$_5$ A$_6$ T$_7$ T$_8$ T$_9$ G$_{10}$ C$_{11}$ G$_{12}$-3'
3'-G$_{-1}$C$_{-2}$G$_{-3}$T$_{-4}$T$_{-5}$T$_{-6}$A$_{-7}$A$_{-8}$A$_{-9}$C$_{-10}$G$_{-11}$C$_{-12}$-5'

tamycin)$_4$:**D2**, were observed via ¹H NMR spectroscopy. In accord with the known antiparallel dimeric binding mode of distamycin, neither distamycin:**D2** nor (distamycin)$_3$:**D2** complexes were seen.[24]

Aqueous solutions of distamycin begin to turn yellow in a short time at room temperature. Replacement of the terminal amidine by dimethylpropylamine and terminal formamide by acetamide provides **L1** (Table 1), which is stable in solution. However, the K_3K_4 value for complexation of dsDNA by **L1** is 1000-fold less than that for complexation by distamycin.[23] Attachment of polyamine chains to the central pyrrole ring of **L1** makes up for the poor association of the dimethylpropylamine and acetamide substituents. The K_3K_4 value for complexation of **D1** by the stable **L7** is roughly 100-fold greater than that for complexation by distamycin.

Structural Investigations. Solution structures for several 1-to-1 complexes of MGTs with d(CGCA$_3$T$_3$GCG)$_2$ (**D2**) were determined by two-dimensional nuclear Overhauser effect ¹H NMR spectroscopy and restrained molecular
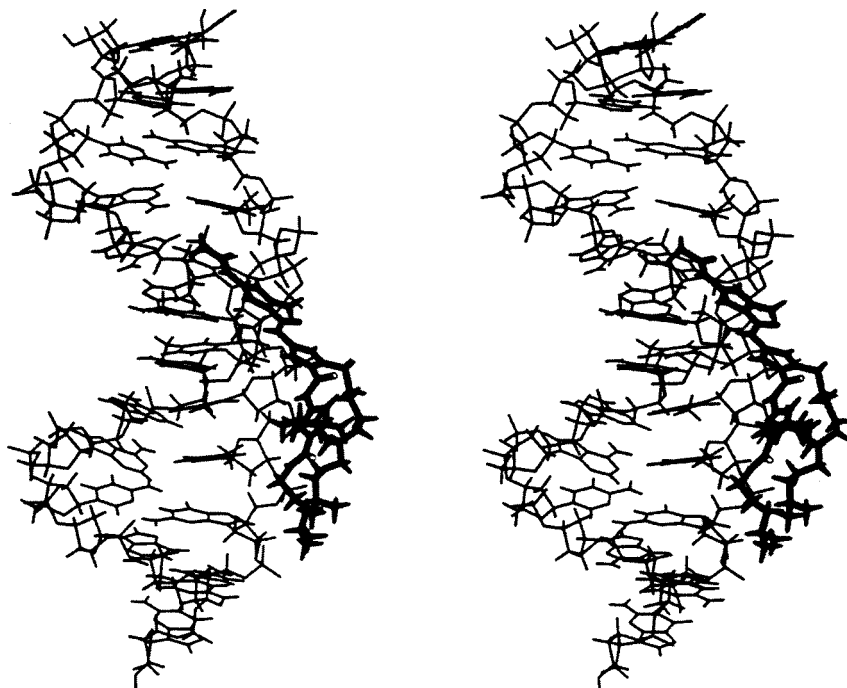
FIGURE 3. Stereo model of the D_2O solution structure of the $d(CGCA_3T_3GCG)_2$:**L5** complex. Microgonotopen **L5** is represented by the bold lines.

modeling. For **L5** (Chart 2), proximities between an N-methyl of the dimethylpropylamine tail and an N-methyl of the bis-dimethylpropylamine side chain with a major groove pointing guanine proton of the dsDNA **D2** ($G_{10}H2''$) show that the tail of the MGT nearly extends out of the minor groove (Figure 3).[26] This requires **L5** to tilt with respect to the minor groove, so that the acetamido end is buried deeper in the minor groove than is the dimethylpropylamine tail end of the molecule. Examination of Figure 3 reveals that the positively charged dimethylpropylamine tail of **L5** resides at a position which is adjacent to the negative phosphodiester P_{11} on the minor groove side of the backbone. Meanwhile, the protonated bis-dimethylpropylamine side chain resides on the major groove side of the DNA backbone and is paired with the phosphodiesters P_8, P_9, and P_{10}. The four protonated amino functions of **L5** possess NH···OP distances ranging from 1.6 to 2.5 Å.

Unlike for **L5**, the dimethylpropylamine tail of **L7** rests deep within the minor groove of **D2** (Figures 4−6).[27] Further, while the amide −(C=O)−NH− nitrogens of **L5** are embedded a distance of 4.5−7.0 Å from the bottom of the minor groove, as traced from the acetamide substituent to the tail end of the molecule, the same nitrogens of **L7** bind 3.1−4.5 Å from the bottom of the groove. The efficiency of binding of the tren amine substituent of **L7** (as seen by the embedding of the tripyrrole peptide in the minor groove) versus that of the bis-dimethylpropylamine substituent of **L5** can be ascribed to the smaller steric effect around the terminal amino groups of the tren substituent, allowing a better pairing with the phosphate backbone of dsDNA.

On chelation of Zn(II), the protonated tren amine substituent of **L7** (i) remains targeted for the P_9 and P_{10}

phosphodiester linkages, (ii) brings about a 2 Å decrease in the P_9−P_{10} distance, and (iii) increases the bending angle in the **L7**:Zn(II):**D2** complex by 14.6° as compared with that in the **L7**:**D2** complex (Figure 6).[28] This bending angle for the **L7**:Zn(II):**D2** complex is comparable to that observed for cisplatin dsDNA complexes (∼36°).[29]

Atomic Force Microscopy. The electrophoretic mobilities of dsDNA restriction fragments are retarded in the presence of MGTs **L3**−**L9**, while they are little affected by distamycin or Hoechst 33258.[21,22,25] The ability to retard dsDNA migration decreases in the order **L8** ∼ **L7** ∼ **L6** > **L3** ∼ **L4** ≫ distamycin > Hoechst 33258. Neither **L1** (which lacks a basic side chain) nor tren amine, on its own, alters the electrophoretic mobility of dsDNA fragments.[30] Further, the MGTs more substantially decrease the mobility of the dsDNA restriction fragments as the size of the fragments increases. This suggests that the binding of the MGTs to A + T-rich sites changes the dsDNA conformation at these sites and that a critical number of sites are required before conformational changes manifest themselves.

To explain the retardation of dsDNA migration by the MGTs, a change in DNA conformation upon ligand binding was proposed. However, in the absence of visual evidence, it was not known whether the conformational change was due to the stiffening, unwinding, physical lengthening, or dsDNA bending (it has been proposed that bent DNAs are retarded in gels because they have a larger effective diameter than linear DNAs). Atomic force microscopy (AFM) images provide direct visual proof that the MGT-induced decrease in the electrophoretic mobility is due to bending of the dsDNA.[30] Randomly selected M400 dsDNA molecules in the absence and in the presence of the MGT **L7** are displayed in Figure 7 by employ-
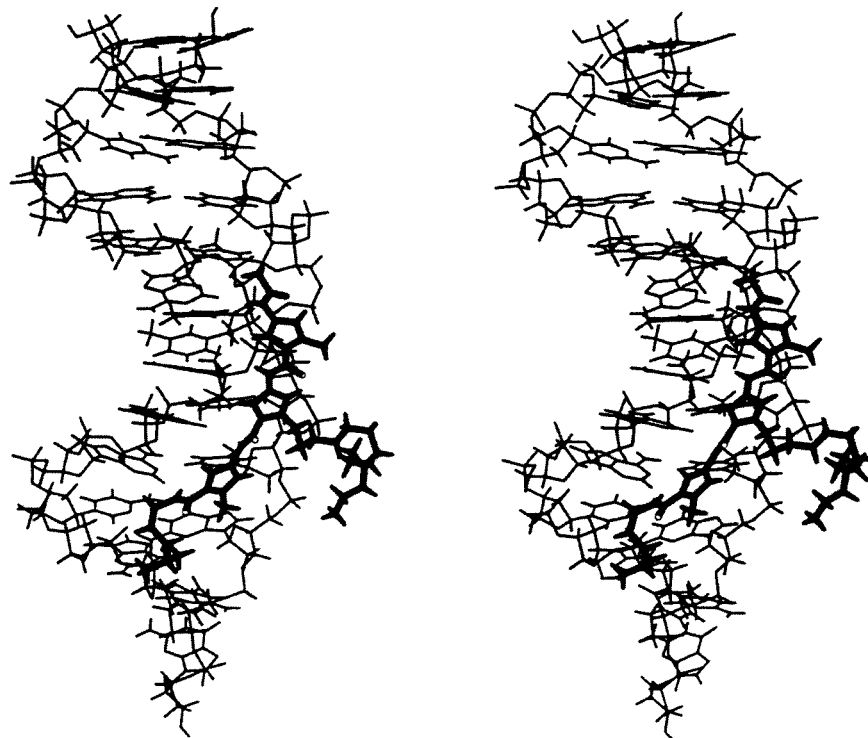
FIGURE 4. Stereo model of the D_2O solution structure of the d(CGCA$_3$T$_3$GCG)$_2$:**L7** complex. Microgonotropen **L7** is represented by the bold lines.
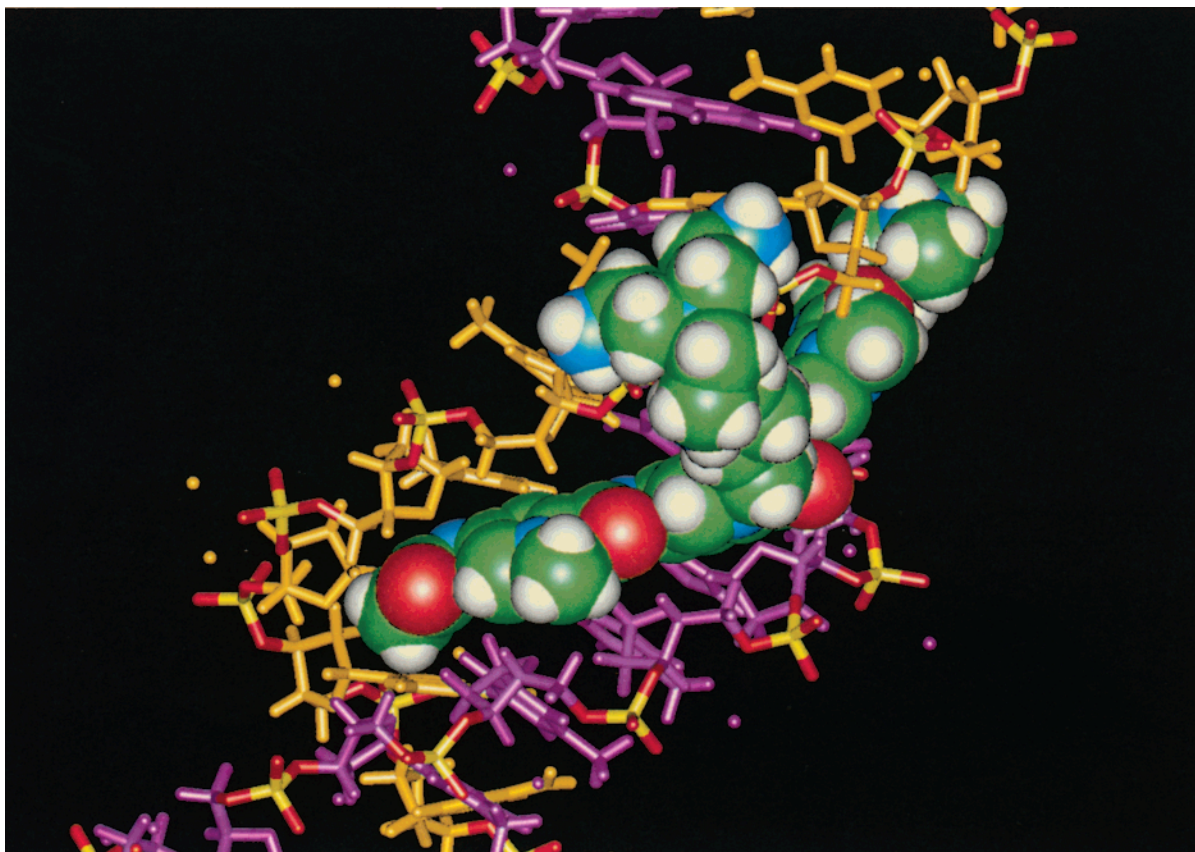
FIGURE 5. Close-up of the d(CGCA$_3$T$_3$GCG)$_2$:**L7** complex.

ing AFM (M400 dsDNA is commonly used as a molecular weight standard for gel electrophoresis and possesses seven A + T-rich binding sites). In the presence of **L7**, the M400 DNA molecules possess conformations of greater curvature or bending. Many of the M400 molecules possess a "hairpin" or a "circular" appearance.
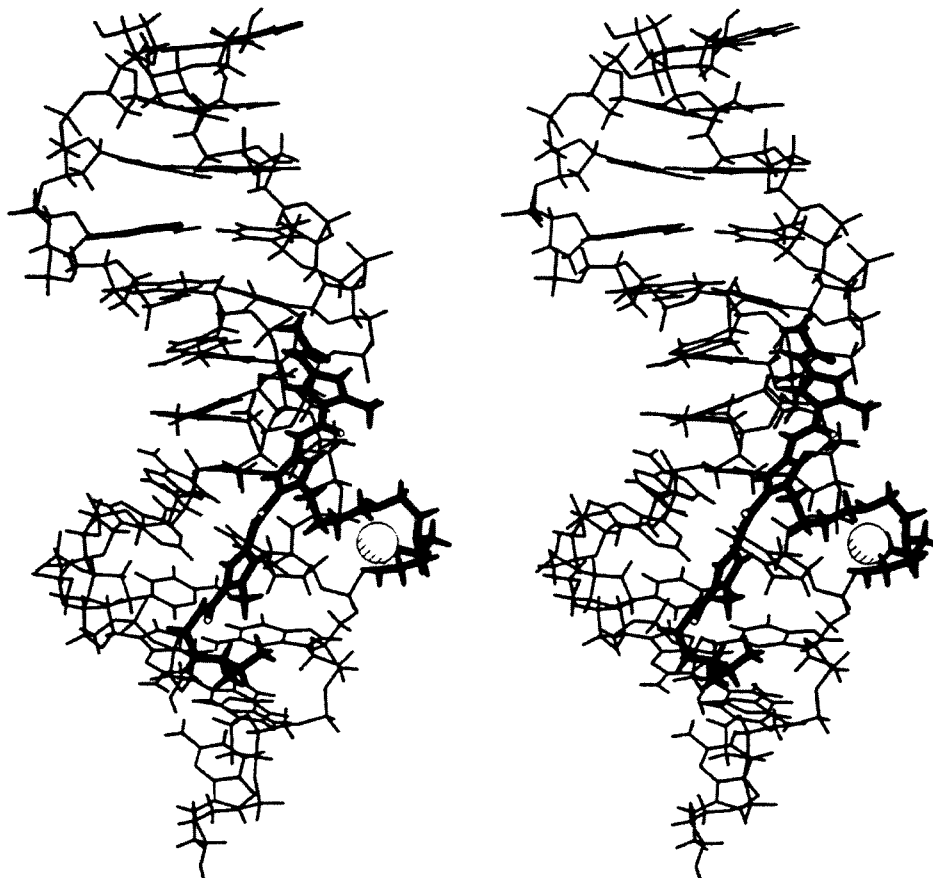
FIGURE 6. Stereo model of the D$_2$O solution structure of the d(CGCA$_3$T$_3$GCG)$_2$:**L7**:Zn(II) complex. Microgonotropen **L7** is represented by the bold lines, while the zinc ion is represented as a van der Waals sphere.
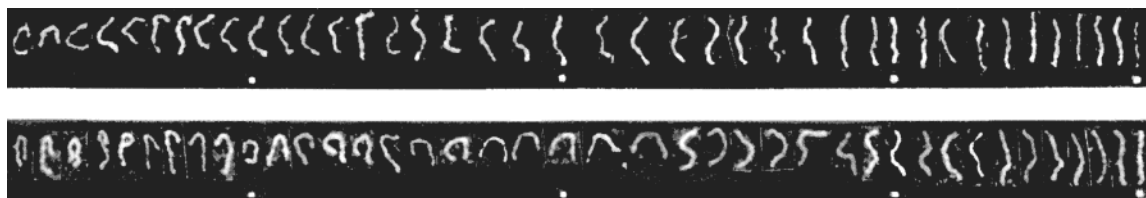

FIGURE 7. Forty molecules of M400 DNA, randomly selected, without (A, top) and with (B, bottom) **L7** at a concentration of 1 molecule of **L7** per 1.4 bp. Molecules are arranged in the order of decreasing bending. Dots mark tens of molecules.
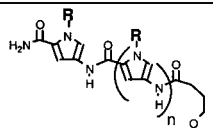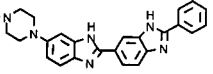
Bisbenzimidazole Microgonotropens
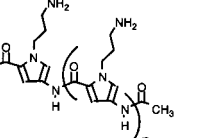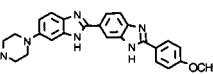
Bisbenzimidazoles bearing the four side chains, tren amine (**L11**), spermine (**L12**), and tri- and penta-arginine (**L13** and **L14**, respectively), were synthesized (Table 2).[31,32] Bisbenzimidazoles fluoresce upon complexation in the minor groove of A + T-rich dsDNA. Thus, stoichiometries and association constants for formation of dsDNA complexes with **L11**, **L12**, **L13**, and **L14** were determined via spectrofluorometric titrations.

Increases in the thermal melting temperature of d(GCGACTGCA$_2$T$_3$CGACGTCC)/d(GGACGTCGA$_3$T$_2$GCAG-TCGC) (**D3**) in the presence of bisbenzimidazole MGTs are shown in Table 2.[31] The large increases in t_m values indicate that **L11**−**L14** possess apparent association constants for complexation of dsDNA several orders of magnitude greater than the association constant of **L10**, which lacks a positively charged protonated amine side chain.

Spectrofluorometric titrations established that the different MGT-**D3** complexes possessed different stoichiometries. **L12** and **L14** form (**L**)$_3$:**D3** complexes, whereas **L10**, **L11**, and **L13** all form (**L**)$_2$:**D3** complexes. The isothermal binding curve generated upon titration of **D3** with **L10** indicates that the two molecules of **L10** in the (**L10**)$_2$:**D3** complex bind **D3** in a cooperative manner (the binding curve possesses an "S" shape). Similar "S"-shaped binding curves are observed for the MGTs **L11**−**L14**. In contrast, Hoechst 33258 forms only a 1-to-1 complex with **D3**.

In agreement with known characteristics, Hoechst 33258 complexes **D3** via a "simple" 1-to-1 binding motif, as depicted in Figure 1b.[7,15] In contrast, the bisbenzimidazole **L10** complexes dsDNA in a cooperative manner, perhaps via an antiparallel side-by-side binding motif usually characteristic of tripyrrole polyamides (Figure 1A). Thus, the higher order 2-to-1 and 3-to-1 stoichiometries observed for **L11**, **L12**, **L13**, and **L14** are in part due to

Table 3. Apparent Association Constants between the dsDNAs D4 and D5 and Heterodimers in H$_2$O, 10 mM Phosphate Buffer, pH 7.0/150 mM NaCl (see Chart 1 for dsDNA sequences)^a

structure		logK^{D4}	logK^{D5}	$\frac{K^{D5}}{K^{D4}}$
R = -CH$_2$(CH$_2$)$_2$NH$_2$	L15, (n = 2)	9.2	12.9	4700
	L16, (n = 1)	8.3	11.1	630
R = -CH$_3$	L17, (n =2)	6.5	9.8	1700
	L18, (n = 2)	8.5	9.6	13
	L19, (n = 1)	6.9	nd	nd
	Hoechst 33377	7.3	7.6	2
	distamycin	7.3	7.8	3

^{a} Apparent association constants were calculated from ligand–dsDNA complex melting temperatures.[37] nd = not determined.

Table 4. Relative Association Constants for Complexation of D6 and Related dsDNAs Containing (A/T) → (G/C) Base Pair Substitutions within the A + T-Rich Binding Site of D6 by Heterodimers (H$_2$O, 10 mM Phosphate Buffer, pH 7.0/150 mM NaCl)

dsDNAs^a	L17^b	L15^c	Ht^b
5′-GCGGTATAAAAATTCGACG-3′ (D6)	1	1	1
5′-GCGG**C**ATAAAATTCGACG-3′ (D7)	0.037	0.18	
5′-GCGGT**G**TAAAATTCGACG-3′ (D8)	0.025	0.019	
5′-GCGGTA**C**AAAATTCGACG-3′ (D9)	0.024	0.0058	
5′-GCGGTAT**G**AAATTCGACG-3′ (D10)	0.057	0.044	
5′-GCGGTATA**G**AATTCGACG-3′ (D11)	0.00043	0.034	0.31
5′-GCGGTATAA**G**ATTCGACG-3′ (D12)	0.035	0.021	
5′-GCGGTATAAA**G**TTCGACG-3′ (D13)	0.017	0.024	
5′-GCGGTATAAAA**C**TCGACG-3′ (D14)	0.017	0.24	
5′-GCGGTATAAAAT**C**CGACG-3′ (D15)	0.035	0.26	
5′-GCGGTATA**GG**AATTCGCG-3′ (D16)	0.00005	0.0056	0.73

^{a} The A + T-rich regions are underlined. (A/T) → (G/C) base pair substitutions are in bold type. ^{b} Stoichiometries of L17 and Hoechst 33258 complexes with dsDNA are 2-to-1. K_1K_2 for complexation of D6 by L17 and by Hoechst 33258 are 3.7 × 10^{18} and 5.6 × 10^{17} M^{-2}, respectively (Scheme 1). The association constants K_1 and K_2 were determined by fitting of an isothermal binding curve generated by spectrofluorometric titration at 26 °C. ^{c} Stoichiometries of dsDNA complexes with L15 are 1-to-1. Apparent association constants for L15–dsDNA complexes were determined via thermal melting investigations. K_1 for complexation of D6 by L15 is 1.6 × 10^{12} M^{-1}.

replacement of the para-hydroxy of Hoechst 33258 with the meta-phenyl ether of L10.

Heterodimeric Molecules

It is expected that those agents capable of recognizing longer dsDNA sequences will also exhibit the greatest specificity.[33–36] We designed an agent, L17, capable of distinguishing longer A + T-rich binding sites from shorter ones (Tables 3 and 4).[12] As shown in Table 4, L17 is selective for its preferred nine A + T base pair binding site as contained within d(GCGGTATA$_4$TTCGACG)/d(C-GTCGAAT$_4$ATACCGC) (D6). Single (A/T) → (G/C) substitutions within the A + T-rich binding site of D6 cause significant decreases in K_1K_2 values for dsDNA complexation (see Scheme 1 for the definition of the association constants K_1 and K_2). In contrast, Hoechst 33258 shows little selectivity for longer dsDNA binding sites because it is not long enough to recognize sequences of more than four DNA base pairs.

Molecular Modeling.[12] All 11 of the dsDNA duplexes investigated (Table 4) were determined to form (ligand)$_2$: dsDNA complexes with L17 and Hoechst 33258. However, the structures of the (L17)$_2$:dsDNA and (Hoechst 33258)$_2$: dsDNA complexes are quite different. The observed 2-to-1 stoichiometries for dsDNA complexes with L17 suggest the formation of antiparallel side-by-side complexes, as depicted in Figure 8. Note the ability of L17 to conform to the curvature of the minor groove of DNA. The antiparallel side-by-side complex of L17 with dsDNA has precedence since monocationic minor groove binders have a propensity to complex dsDNA in this manner (see Figure 1A). Placing the bisbenzimidazole moiety of one L17 molecule adjacent to the tripyrrole moiety of the second L17 molecule in an antiparallel arrangement avoids placement of the bulky and positively charged piperizine rings against one another. Also, slightly staggering the two L17 molecules avoids placing the terminal primary amide of one L17 molecule adjacent to the bulky piperazine ring of the other. Staggering the molecules is especially reasonable since structural investigations of side-by-side complexes of tripyrrole polyamides with dsDNA consistently show the two molecules to be both antiparallel and staggered.[15] Consistent with known characteristics, each Hoechst 33258 molecule in a (Hoechst 33258)$_2$:dsDNA complex resides in a four A + T base pair region, similar to the "simple" 1-to-1 binding motif depicted in Figure 1B, such that the two Hoechst molecules are arranged end-to-end and do not overlap each other.

Heterodimeric Microgonotropens.[37] We sought to explore dsDNA binding agents which would specifically recognize longer DNA sequences while also possessing the superior transcription factor inhibitory activity of the monomeric tripyrrole and bisbenzimidazole microgonotropens (Tables 1 and 2). L15 is an example of such an agent (Table 3) and was prepared by replacing the pyrrole N-methyl substituents of L17 with propylamine chains. Model building demonstrated how L15 could adapt a "spiral-like" conformation which matched that of the dsDNA minor groove—much as seen in the structure of L17 in Figure 8.[37]

L15 is observed to form 1-to-1 complexes with dsDNAs D5 and D6, both of which possess nine base pair A + T-rich binding sites, at subpicomolar concentrations (see Chart 1 for DNA sequences). For L15, the K_1 for complexation of d(CGCA$_9$CGC)/d(GCGT$_9$GCG) (D5) is 5000-fold greater than that for complexation of d(CGCA$_5$CGCACC)/ d(GGTGCGT$_5$GCG) (D4), whereas Hoechst 33342 and distamycin demonstrate no significant preference for either D5 or D4 (Table 3). The specificity of L15 was

FIGURE 8. Computer-generated model of the proposed (**L17**)₂:dsDNA side-by-side antiparallel staggered complex.

further investigated by employing **D6** and its derivatives **D7**–**D16** (Table 4). Single base pair substitutions near the center of the A + T-rich region of **D6** led to significant 20–200-fold decreases in K_1. Thus, the overall effect of the propylamine chains is to strengthen **L15**–dsDNA interactions without a loss of sequence specificity.

Biological Activity

E2 factor (E2F), first defined as a cellular DNA-binding protein required for transactivation of the adenovirus E2 promoter, is known to participate in cell growth control.[38]

Table 5. Inhibition of E2F1—DNA Complex Formation by Tripyrrole Polyamides[a]

agent	relative activity
Dm	1.0
L2	4.6
L3	6.3
L6	4500
L7	2700
L8	49
L9	2400

[a] Relative activity was normalized by comparing the IC₅₀ of individual drugs to that of distamycin (**Dm**).

E2F1 (the first E2F family member) binds to adjacent A + T and G + C-rich sequences, and its binding affects both grooves of DNA.[3,39] Beerman and co-workers have investigated the ability of tripyrrole MGTs to prevent complex formation between E2F1 and its consensus dsDNA binding site via electrophoretic mobility shift assays.[3] The relative activities of the MGTs, compared to those of distamycin, are listed in Table 5. The most effective inhibitor of TF—DNA complex formation, **L6**, shows an almost 5000-fold increase in activity over distamycin (the IC₅₀ of **L6** is 0.00085 μM).

L6 also showed more potent activity toward NF-κB, a ubiquitous transcription factor thought to be a regulator of early response genes.[40] NF-κB primarily contacts its dsDNA binding site, which contains an A + T-rich region, through the major groove.[41] Mobility shift assays conducted by Bruice and Kwok showed **L6** to possess an IC₅₀ of less than 5 nM, making it 6000-fold more potent than distamycin.[42]

Beerman and co-workers also investigated the ability of bisbenzimidazole MGTs to inhibit formation of a transcription factor complex with the human c-fos serum response element (SRE).[43] The complexation of an A +T-rich site within the SRE by a homodimer of the TF serum response factor (SRF) is required for recruitment of a second transcription factor, Elk-1, to a GGA-containing ets motif within the SRE.[44] Both TFs primarily contact their consensus sequences in the major groove, but some contacts are also made within the minor groove. Cell-free mobility shift assays showed that **L10**, which lacks a positively charged side chain, showed no inhibitory activity, while the MGTs **L11**–**L14** all possessed IC₅₀ values in the micromolar range. Hence, the functionalization of **L10** with a positively charged side chain is necessary for inhibitory activity.

Similar to the monomeric MGTs, the heterodimeric MGTs possessed a superior ability to disrupt TF—dsDNA interactions in cell-free assays.[45] Again, the positively charged side chain of the MGT was shown to be necessary for TF inhibitory activity. **L17**, which lacks the side chains of **L15**, possesses a relative inhibitory activity at least 3 orders of magnitude less than that of **L15** (see Table 6). More so, **L15**, unlike the previously discussed monomeric MGTs, demonstrated the ability to inhibit gene expression in whole cells. The IC₅₀ for inhibition of c-fos expression by **L15** in NIH3T3 cells was 9 μM. Thus, **L15** is unique among the MGTs in that it can traverse the cell membrane and reach its nuclear DNA target.

Table 6. Inhibition of Ternary Complex Formation by Heterodimers[a]

agent	relative activity
Ht 33342	1.0
L15	120
L16	40
L17	<0.48
L18	15
L19	0.44

[a] Relative activity was normalized by comparing the IC_{50} of individual drugs to that of Hoechst 33342. The IC_{50} for **L15** is 0.041 μM.

Binding studies show that the bulk of free energy of dsDNA binding by **L15** stems from the molecule's tripyrrole and not its bisbenzimidazole moiety (Table 3). Further, **L18**, which is representative of the tripyrrole moiety of **L15**, possesses a TF inhibitory activity nearly equal to that of **L15** in cell-free assays (Table 6). Thus, in cell-free assays the tripyrrole moiety of **L15** confers upon the heterodimer both binding "strength" and TF inhibitory activity, while the bisbenzimidazole moiety is necessary for sequence specificity and whole cell activity.

Conclusions

Attachment of protonated and positively charged alkyl-amine side chains to the tripyrrole (**L1**), bisbenzimidazole (**L10**), and heterodimer (**L17**) turns these otherwise ineffective minor groove binding molecules (MGBs) into potent inhibitors of transcription factor (TF)–dsDNA interactions (Tables 1–3). We call this new class of minor groove binding molecules "microgonotropens" (MGTs). The superior ability of MGTs to inhibit the binding of TFs to their dsDNA binding sites arises from their increased association constants for dsDNA complexation, bending of the dsDNA helix upon binding, and neutralization of the negatively charged DNA backbone via electrostatic interaction with their positively charged side chains. While tripyrrole and bisbenzimidazole MGTs (Tables 1 and 2) showed promising cell-free TF inhibitory activities, they possessed little activity in whole cells, probably due to a failure to traverse the cell membrane or a propensity to react with biological molecules other than nuclear DNA. However, the heterodimer **L15** (Table 3) inhibits gene expression in whole cells at micromolar concentrations.

The long-term goal of controlling the expression of specific genes in a cell is unattainable with agents that recognize short DNA sequences of four or five base pairs. Thus, we have developed MGBs which recognize longer dsDNA binding sites. Particularly, we have found that the longer molecules **L15** and **L17** (Table 3) are capable of recognizing binding sites up to nine base pairs long with high sequence specificity. These molecules adapt a spiral conformation which allows them to wrap around nearly a full turn of the dsDNA helix (Figure 8).

While microgonotropens demonstrate a promising combination of sequence specificity and TF inhibitory activity, they still fall short of achieving selective gene control in vivo. An interesting approach for future work includes the development of more advanced major groove contacting moieties for the microgronotropens. The polyamine chains of the existing microgonotropens possess no specificity. Microgonotropens possessing moieties capable of sequence-specific interactions in the major groove should yield superior drug candidates.

References

(1) Latchman, D. S. *Gene regulation: a eukaryotic perspective*, 3rd ed.; Stanley Thornes: Cheltenham, 1998.

(2) Chiang, S. Y.; Welch, J.; Rauscher, F. J.; Beerman, T. A. Effects of Minor Groove Binding Drugs on the Interaction of Tata Box Binding Protein and TFIIa with DNA. *Biochemistry* **1994**, *33*, 7033–7040.

(3) Chiang, S. Y.; Bruice, T. C.; Azizkhan, J. C.; Gawron, L.; Beerman, T. A. Targeting E2F1-DNA Complexes with Microgonotropen DNA Binding Agents. *Proc. Natl. Acad. Sci. U.S.A.* **1997**, *94*, 2811–2816.

(4) Gottesfeld, J. M.; Neely, L.; Trauger, J. W.; Baird, E. E.; Dervan, P. B. Regulation of Gene Expression by Small Molecules. *Nature* **1997**, *387*, 202–205.

(5) Praseuth, D.; Guieysse, A. L.; Helene, C. Triple Helix Formation and the Antigene Strategy for Sequence-Specific Control of Gene Expression. *Biochim. Biophys. Acta–Gene Struct. Express.* **1999**, *1489*, 181–206.

(6) Satz, A. L.; White, C. M.; Beerman, T. A.; Bruice, T. C. Double-Stranded DNA Binding Characteristics and Subcellular Distribution of a Minor Groove Binding Diphenyl Ether Bisbenzimimidazole. *Biochemistry* **2001**, *40*, 6465–6474.

(7) Reddy, B. S. P.; Sondhi, S. M.; Lown, J. W. Synthetic DNA minor groove-binding drugs. *Pharmacol. Ther.* **1999**, *84*, 1–111.

(8) Boger, D. L.; Garbaccio, R. M. Shape-dependent catalysis: Insights Into the Source of Catalysis for the CC-1065 and Duocarmycin DNA Alkylation Reaction. *Acc. Chem. Res.* **1999**, *32*, 1043–1052.

(9) Lammler, G.; Herzog, H.; Saupe, E.; Schutze, H. R. Chemotherapeutic Studies on *Litomosoides carinii* Infection of *Mastomys natalennsis*. *WHO Bull.* **1971**, *44*, 751–756.

(10) Harshman, K. D.; Dervan, P. B. Molecular recognition of B-DNA by Hoechst 33258. *Nucleic Acids Res.* **1985**, *13*, 4825–4835.

(11) Baird, E. E.; Dervan, P. B. Solid-Phase Synthesis of Polyamides Containing Imidazole and Pyrrole Amino Acids. *J. Am. Chem. Soc.* **1996**, *118*, 6141–6146.

(12) Satz, A. L.; Bruice, T. C. Recognition of Nine Base Pairs in the Minor Groove of DNA by a Tripyrrole Peptide-Hoechst Conjugate. *J. Am. Chem. Soc.* **2001**, *123*, 2469–2477.

(13) Latt, S. A.; Wohlleb, J. C. Optical studies of the Interaction of Hoechst 33258 with DNA, Chromatin, and Metaphase Chromosomes. *Chromosoma* **1975**, *52*, 297–316.

(14) Teng, M.-K.; Usman, N.; Frederick, C. A.; Wang, A. H.-J. The Molecular Stucture of the Complex of Hoechst 33258 and the DNA Dodecamer d(CGCGAATTCGCG). *Nucleic Acids Res.* **1988**, *16*, 2671–2690.

(15) Wemmer, D. E. Designed Sequence-Specific Minor Groove Ligands *Annu. Rev. Biophys. Biomol. Struct.* **2000**, *29*, 439–461.

(16) Neidle, S. Crystallographic Insights into DNA Minor Groove Recognition by Drugs. *Biopolymers* **1997**, *44*, 105–121.

(17) Wiederholt, K.; Rajur, S. B.; McLaughlin, L. W. Oligonucleotides Tethering Hoechst 33258 Derivatives: Effect of the Conjugation Site on Duplex Stabilization and Fluorescence Properties. *Bioconjugate Chem.* **1997**, *8*, 119–126.

(18) Oakley, M. G.; Mrksich, M.; Dervan, P. B. Evidence That a Minor Groove-Binding Peptide and a Major Groove-Binding Protein Can Simultaneously Occupy a Common Site on DNA. *Biochemistry* **1992**, *31*, 10969–10975.

(19) Sondhi, S. M.; Magan, A.; Lown, J. W. Synthesis of a Series of Acodazole and Naphthothiophene-Deuterioporphyrins and Metalloporphyrins. *Bull. Chem. Soc. Jpn.* **1992**, *65*, 579–585.

(20) Bruice, T. C.; Mei, H. Y.; He, G. X.; Lopez, V. Rational Design of Substituted Tripyrrole Peptides that Complex with DNA by Both Selective Minor-Groove Binding and Electrostatic Interaction with the Phosphate Backbone. *Proc. Natl. Acad. Sci. U.S.A.* **1992**, *89*, 1700–1704.

(21) He, G. X.; Browne, K. A.; Groppe, J. C.; Blasko, A.; Mei, H. Y.; Bruice, T. C. Microgonotropens and Their Interactions with DNA. 1. Synthesis of the Tripyrrole Peptides Dien-Microgonotropen-a, Dien-Microgonotropen-b, and Dien-Microgonotropen-c and Characterization of Their Interactions with dsDNA. *J. Am. Chem. Soc.* **1993**, *115*, 7061–7071.

(22) He, G. X.; Browne, K. A.; Blasko, A.; Bruice, T. C. Microgonotropens and Their Interactions with DNA. 4. Synthesis of the Tripyrrole Peptides Tren-Microgonotropen-a and -b and Characterization of Their Interactions with dsDNA. *J. Am. Chem. Soc.* **1994**, *116*, 3716–3725.

(23) Browne, K. A.; He, G. X.; Bruice, T. C. Microgonotropens and Their Interactions with DNA. 2. Quantitative Evaluation of Equilibrium Constants For 1:1 and 2:1 Binding of Dien-Microgonotropen-a, Dien-Microgontropen-b, and Dien-Microgontropen-d as well as Distamycin and Hoechst 33258 to d(GGCGAAATTTGGCGG)/d(CCGCCAAATTTGCGCC). *J. Am. Chem. Soc.* **1993**, *115*, 7072–7079.

(24) Blasko, A.; Bruice, T. C. Stoichiometry and Structure of Complexes of DNA Oligomers with Microgonotropens and Distamycin By H[1] NMR Spectroscopy and Molecular Modeling. *Proc. Natl. Acad. Sci. U.S.A.* **1993**, *90*, 10018–10022.

(25) Sengupta, D.; Blasko, A.; Bruice, T. C. A Microgonotropen Pentaaza Pentabutylamine and its Interactions with DNA. *Bioorg. Med. Chem.* **1996**, *4*, 803–813.

(26) Blasko, A.; Browne, K. A.; He, G. X.; Bruice, T. C. Microgonotropens and Their Interactions with DNA. 3. Structural Analysis of the 1:1 Complex of d(CGCAAATTTGCG)$_2$ and Dien-Microgonotropen-c by 2D NMR Spectroscopy and Restrained Molecular Modeling. *J. Am. Chem. Soc.* **1993**, *115*, 7080–7092.

(27) Blasko, A.; Browne, K. A.; Bruice, T. C. Microgonotropens and Their Interactions with DNA. 5. Structural Characterization of the 1:1 Complex of d(CGCAAATTTGCG)$_2$ and Tren-Microgonotropen-b by 2D NMR Spectroscopy and Restrained Molecular Modeling. *J. Am. Chem. Soc.* **1994**, *116*, 3726–3737.

(28) Blasko, A.; Browne, K. A.; Bruice, T. C. NMR Structure of d(CGCAAATTTGCG)$_2$:Tren-Microgonotropen-b:Zn(II) Complex and Solution Studies of Metal Ion Complexes of Tren-Microgonotropen-b Interacting with DNA. *Bioorg. Med. Chem.* **1995**, *3*, 631–646.

(29) Yang, D. Z.; Wang, A. H. J. Structural Studies of Interactions Between Anticancer Platinum Drugs and DNA. *Prog. Biophys. Mol. Biol.* **1996**, *66*, 81–111.

(30) Hansma, H. G.; Browne, K. A.; Bezanilla, M.; Bruice, T. C. Bending and Straightening of DNA Induced by the Same Ligand—Characterization With the Atomic Force Microscope. *Biochemistry* **1994**, *33*, 8436–8441.

(31) Satz, A. L.; Bruice, T. C. Synthesis of Fluorescent Microgonotropens (FMGTs) and Their Interactions with dsDNA. *Bioorg. Med. Chem.* **2000**, *8*, 1871–1880.

(32) Satz, A. L.; Bruice, T. C. Synthesis of a Fluorescent Microgonotropen (FMGT-1) and its Interactions with the Dodecamer d(CCGGAATTCCGG)$_2$. *Bioorg. Med. Chem. Lett.* **1999**, *9*, 3261–3266.

(33) Kissinger, K. L.; Dabrowiak, J. C.; Lown, J. W. Molecular Recognition Between Oligopeptides and Nucleic Acids—DNA Binding Specificity of a Series of Bis Netropsin Analogues Deduced From Footprinting Analysis. *Chem. Res. Toxicol.* **1990**, *3*, 162–168.

(34) Trauger, J. W.; Baird, E. E.; Dervan, P. B. Recognition of 16 Base Pairs in the Minor Groove of DNA by a Pyrrole-Imidazole Polyamide Dimer. *J. Am. Chem. Soc.* **1998**, *120*, 3534–3535.

(35) Trauger, J. W.; Baird, E. E.; Mrksich, M.; Dervan, P. B. Extension of Sequence-Specific Recognition in the Minor Groove of DNA By Pyrrole-Imidazole Polyamides to 9–13 Base Pairs. *J. Am. Chem. Soc.* **1996**, *118*, 6160–6166.

(36) Kelly, J. J.; Baird, E. E.; Dervan, P. B. Binding Site Size Limit of the 2:1 Pyrrole-Imidazole Polyamide-DNA Motif. *Proc. Natl. Acad. Sci. U.S.A.* **1996**, *93*, 6981–6985.

(37) Satz, A. L.; Bruice, T. C. Recognition of Nine Base Pair Sequences in the Minor Groove of DNA at Subpicomolar Concentrations by a Novel Microgonotropen. *Bioorg. Med. Chem.* **2002**, *10*, 241–262.

(38) Slansky, J. E.; Farnham, P. J. Introduction to the E2F Family: Protein Structure and Gene Regulation. *Curr. Top. Microbiol. Immun.* **1996**, *208*, 1–30.

(39) Bruice, T. C.; Sengupta, D.; Blasko, A.; Chiang, S. Y.; Beerman, T. A. A Microgonotropen Branched Decaaza Decabutylamine and its DNA and DNA/Transcription Factor Interactions. *Bioorg. Med. Chem.* **1997**, *5*, 685–692.

(40) Baeuerle, P. A.; Henkel, T. Function and Activation of NF-κB in the Immune System. *Annu. Rev. Immunol.* **1994**, *12*, 141–179.

(41) Chen, F. E.; Huang, D. B.; Chen, Y. Q.; Ghosh, G. Crystal structure of p50/p65 Heterodimer of Transcription Factor NF-κB bound to DNA *Nature* **1998**, *391*, 410–413.

(42) Bruice, T. W.; Kwok, Y. Unpublished results.

(43) White, C. M.; Satz, A. L.; Gawron, L. S.; Bruice, T. C.; Beerman, T. A. Inhibiting Transcription Factor/DNA Complexes using Fluorescent Microgonotropens (FMGTs). *Biophys. Biochim. Acta*, in press.

(44) Treisman, R. The Serum Response Element. *Trends Biochem. Sci.* **1992**, *17*, 423–426.

(45) White, C. M.; Satz, A. L.; Bruice, T. C.; Beerman, T. A. Inhibition of Transcription Factor—DNA Complexes and Gene Expression by Novel Microgonotropens that Interact with Both Grooves of DNA. *Proc. Natl. Acad. Sci. U.S.A.* **2001**, *98*, 10590–10595.